PERGAMON

International Journal of Heat and Mass Transfer 45 (2002) 723–733

International Journal of HEAT and MASS TRANSFER

www.elsevier.com/locate/ijhmt

Development of tree-shaped flows by adding new users to existing networks of hot water pipes

W. Wechsatol [a], S. Lorente [b], A. Bejan [a,*]

[a] *Department of Mechanical Engineering and Materials Science, School of Engineering, Box 90300, Duke University, Durham, NC 27708-0300, USA*

[b] *Department of Civil Engineering, National Institute of Applied Science (INSA), 135 Avenue de Rangueil, Toulouse 31077, France*

Received 19 February 2001; received in revised form 7 June 2001

Abstract

This paper describes the optimization of a tree-shaped system of insulated pipes for the distribution of a stream of hot water over an area. The area is covered uniformly by users who must receive the same flow rate of hot water. The network of pipes is developed in steps. Each step consists of attaching to an existing network an extension (one new user) that is placed in the position that maximizes the temperature of the water received by the new user. The network grows 'one-by-one', i.e., by one new user at a time. Networks with up to 16 users are optimized in this manner, and their geometric features and thermo-fluid performance are documented. These one-by-one trees of hot water flows are compared with corresponding 'constructal' trees that are obtained in steps of pairing (doubling), i.e., connecting together two identical area constructs of the same size. It is shown that although the constructal trees perform the best (uniform water delivery at the highest temperature), the one-by-one trees approach the same level of performance as they become more complex. It is also shown that the geometry of the insulated tree structure is relatively insensitive to how the insulation is distributed over all the pipes. The thermal performance of the structure is relatively insensitive to how finely the distribution of pipe sizes and insulation radii is optimized.

Keywords: Constructal design; Tree networks; Thermal insulation; Topology; Optimization

1. Morphing flow structures with improving performance

In this paper we take a new look at the fundamental heat and fluid flow problem of how to connect optimally and deterministically a finite size volume and one point (source, or sink). This problem has many and diverse applications that go beyond the field of heat transfer and fluids engineering, for example in physiology, river morphology, and electrical engineering [1–5]. In heat transfer, the main application is in miniaturized devices where cooling can be provided only by conduction. The trend toward smaller sizes and conduction-cooling at the smallest scales is illustrated in the recent reviews of the field [6–8].

It is well-known that the geometric configuration of a flow can be optimized (i.e., arranged, distributed in space) so that the global performance of the flow system is maximized. For example, the optimization of the architecture of assemblies of heat-generating components is an essential feature of many of the more recent contributions to the cooling of electronics [9–11]. In the optimization of the volume-to-point path for heat flow [12] it was shown that a volume subsystem of any size can have its external shape and internal details optimized such that its own volume-to-point resistance is minimal. This principle is repeated in the optimization of volumes of increasingly larger scales, where each new volume is an assembly of previously optimized smaller volumes. The construction spreads, as the assemblies cover larger spaces. This approach, which serves as starting point for the present paper was named constructal design [1], and is illustrated in Section 2.

* Corresponding author. Tel.: +1-919-660-5309; fax: +1-919-660-8963.

E-mail address: dalford@duke.edu (A. Bejan).

0017-9310/02/$ - see front matter
PII: S0017-9310(01)00200-9

Nomenclature

A_i	area covered by the doubling construct of level i, m^2 (Fig. 1)
c_p	specific heat at constant pressure, J kg^{-1} K^{-1}
f	friction factor
k	thermal conductivity, W m^{-1} K^{-1}
L_0	side of elemental square area, m
$\dot{m}$	mass flow rate, kg s^{-1}
N_0	number of heat loss units, Eq. (5)
q'	heat transfer rate per unit length, W m^{-1}
r_i	insulation inner radius, m
r_o	insulation outer radius, m
R	ratio of insulation radii, r_o/r_i
T	temperature, K
T_{end}	end temperature, K
T_i	temperature of the water received by the ith user, K
T_∞	ambient temperature, K
V	volume, m^3
$\tilde{V}$	dimensionless volume, Eqs. (12) and (14)
$\dot{W}_0$	elemental pumping power, W

Greek symbols

ΔP	pressure drop, Pa
ρ	density, kg m^{-3}
θ	dimensionless temperature, Eqs. (11) and (13)

Subscripts

0	element
1	first construct
2	second construct

The new approach to the design of tree-shaped flows that forms the subject of this paper is inspired by the spontaneous generation of tree-shaped patterns of traffic in 'urban growth' [13–15]. New neighborhoods are added to existing tree structures. In other words, the new (larger) tree-shaped flow is not optimized again, globally, as a new assembly. Instead, the newcomer is simply grafted onto the tree in the spot that is the most advantageous to the newcomer. We refer to this approach as the "one-by-one tree growth". We follow the growth and evolution of the tree based on this principle, and show that the somewhat irregular tree structure that results has many features in common with the organized, constructal tree design. One such feature is the global performance of the tree flow structure: the one-by-one grown structure performs nearly as well as the constructal structure if the structure is sufficiently large and complex.

We illustrate this new approach by considering the fundamental problem of distributing a supply of hot water as uniformly as possible over a given territory. This is a classical problem of civil engineering, with related subfields in piping networks, sewage and water runoff, irrigation, steam piping, etc. [16–19]. Recent studies of hot water distribution networks are [20–23]. For example, unlike in [22], where the flow path geometry is assumed (frozen) throughout the remaining optimization process, in the present study we reserve the freedom to change the configuration, to "morph" it into better patterns en route to higher levels of performance.

Configuration (geometry, architecture, topology) is the chief unknown and major challenge in design. We illustrate this by reviewing the constructal tree network, and continuing with the development of the one-by-one growth network.

2. Tree network generated by repetitive pairing

The present treatment of the hot water distribution problem is restricted to its thermo-fluid aspects. Considerations of insulation cost and exergetic costs associated with capital and flow irreversibilities [24,25] are left for more advanced models that could be subjected to the approach outlined in this article. The distribution of hot water to users on a specified territory presents two problems to the thermal designer: the fluid mechanics problem of minimizing the pumping power, and the heat transfer problem of minimizing the loss of heat from the piping network, or maximizing the temperature of the water received by each new user that is added to the network (Section 3).

To see what is new in the one-by-one growth mechanism proposed in this paper, it is useful to review the hierarchical structure of the constructal approach. Fig. 1 shows how a two-dimensional territory is supplied with hot water in steps of area sizes that double from one flow structure to the next. The first and smallest is the elemental area of size $A_0 = L_0 \times L_0$, which is supplied by the elemental stream $\dot{m}_0$ of temperature T_0. The elemental length scale L_0 is fixed and assumed to be known. The subsequent constructs ($A_1 = 2L_0^2$, $A_2 = 2^2L_0^2, \ldots$) are obtained by pairing two constructs of the preceding size. The objective is to supply with hot water the users distributed uniformly over A_i, and to accomplish this task with minimal pumping power and a finite amount of thermal insulation. The geometry of each pipe is described by its length (a fraction or multiple of L_0), inner radius wetted by the flow (r_i), and ratio of insulation radii ($R = r_o/r_i$), where r_o and r_i are the outer and inner radii of the insulation shell. This nomenclature is illustrated Fig. 1. The pipe wall thickness is neglected. The subscripts 0, 1, and 2, indicate the elemental area, first

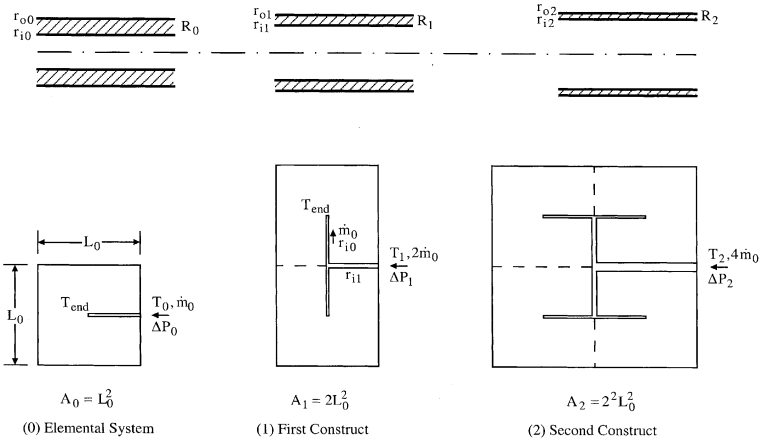

Fig. 1. Sequence of area constructs obtained by pairing smaller constructs.

construct, second construct, etc., in accordance with the notation shown in Fig. 1.

To minimize the pumping power requirement at the elemental level ($\dot{W}_0 = \dot{m}_0 \Delta P_0/\rho$) is to minimize the pressure drop along the elemental duct of the length $L_0/2$. Assuming that the flow is fully developed turbulent in the fully rough regime ($f =$ constant), we find that the pressure drop derived from the definition of friction factor [16,25] is

$$\Delta P_0 = \frac{f}{\pi^2} \frac{\dot{m}_0^2 L_0/2}{\rho r_{i0}^5}. \tag{1}$$

The elemental pressure drop ΔP_0 cannot be minimized geometrically, because it decreases monotonically as the elemental pipe size r_{i0} increases. The incentive to use a minimum amount of insulation at the elemental level, and the availability of pipe sizes that are not smaller than a certain size, justify the assumption that r_{i0} and ΔP_0 are fixed when L_0, $\dot{m}_0$ and the roughness of commercial pipes (f) are specified.

For the analysis of heat loss between the elemental pipe inlet ($T = T_0$ at $x = 0$) and the outlet represented by the user ($T = T_{end}$ at $x = L_0/2$), we write

$$q' = \frac{2\pi k}{\ln(r_o/r_i)}[T(x) - T_\infty], \tag{2}$$

where q', k and T_∞ are the heat loss per unit of pipe length, the thermal conductivity of the insulation shell, and the temperature of the ambient. It is assumed that the thermal resistance between the water stream (T) and the ambient (T_∞) is dominated by the insulation. Combining Eq. (2) with the first law written for the stream of length dx,

$$\dot{m} c_p \, dT = -q' \, dx \tag{3}$$

and integrating from $T = T_0$ at $x = 0$ to $T = T_{end}$ at $x = L_0/2$, we obtain

$$\frac{T_{end} - T_\infty}{T_0 - T_\infty} = \exp\left(-\frac{N_0}{\ln R_0}\right), \tag{4}$$

where, by analogy with the number of heat transfer units (NTU) used in heat exchanger analysis [25], N_0 is the "number of heat loss units" based on elemental quantities

$$N_0 = \frac{\pi k L_0}{\dot{m}_0 c_p}. \tag{5}$$

At the first-construct level (A_1, Fig. 1) there are two pipe sizes, one central pipe of length $(1/2)L_0$ and radii r_{i1} and $R_1 = (r_o/r_i)_1$, and two elemental branches of length $(1/2)L_0$ and radii r_{i0} and $R_0 = (r_o/r_i)_0$. The flow rate is $2\dot{m}_0$ through the root of the tree, and $\dot{m}_0$ through each branch. By writing the equivalent of Eq. (1) for each segment of pipe without branches, we find that the drop in pressure from the root to the most distant user (the center of the farthest element) is

$$\Delta P_1 = \frac{f}{\pi^2} \frac{\dot{m}_0^2 L_0}{\rho} \left(\frac{2}{r_{i1}^5} + \frac{1}{2r_{i0}^5}\right). \tag{6}$$

The pressure drop ΔP_1 can be minimized by selecting the ratio of pipe sizes r_{i1}/r_{i0} subject to a water volume constraint. If we constrain the amount of duct wall material, and if we assume that the duct thickness (t) is a constant independent of duct inner radius, then the constraint means that the total wetted surface is fixed,

$$\frac{1}{2} L_0 r_{i1} + L_0 r_{i0} = \text{constant}. \tag{7}$$

The same geometric relation applies when the constraint refers to the amount of soil that must be excavated in order to bury the pipe system to a constant depth. The minimization of ΔP_1 subject to constraint (7) yields

$$(r_{i1}/r_{i0})_{opt} = 2^{1/2}. \tag{8}$$

An alternative is to constrain the total volume occupied by the ducts,

$$\frac{1}{2}L_0 r_{i1}^2 + L_0 r_{i0}^2 = \text{constant}. \tag{9}$$

This constraint also represents applications where the thickness of each pipe is proportional to the pipe inner radius, and where the total amount of wall material is constrained. In such cases, the minimization of ΔP_1 subject to constraint (9) yields a slightly different optimal step in pipe size,

$$(r_{i1}/r_{i0})_{opt} = 2^{3/7}. \tag{10}$$

For the optimization of the geometry of the thermal insulation shells wrapped around each pipe, we write a temperature drop expression of type (4) for each segment of pipe without branches. We omit the algebra and report only the overall temperature drop from the root of the tree (T_1) to the temperature (T_{end}) of the water stream delivered to the most distant user,

$$\theta_1 = \frac{T_{end} - T_\infty}{T_1 - T_\infty} = \exp\left(-\frac{N_0}{\ln R_0} - \frac{N_0}{2\ln R_1} \right). \tag{11}$$

The dimensionless end temperature θ_1 depends on three parameters, R_0, R_1 and N_0. The geometric parameters R_0 and R_1 are related through the thermal insulation volume constraint

$$\tilde{V}_1 = \frac{V_1}{\pi L_0 r_{i0}^2} = \frac{1}{2}\left(\frac{r_{i1}}{r_{i0}}\right)^2 (R_1^2 - 1) + (R_0^2 - 1) \tag{12}$$

for which (r_{i1}/r_{i0}) is furnished by Eq. (8) or Eq. (10). The maximization of θ_1 with respect to R_0 and R_1, and subject to $\tilde{V}_1 = \text{constant}$ yields the optimal distribution of insulation (Fig. 2(a)) and the maximized end-user water temperature (Fig. 2(b)). The choice of constraint – Eq. (8) (dashed line) versus Eq. (10) (solid line) – has only a small effect, therefore we retain only the duct volume constraint (10) in rest of this paper.

At the second-construct level (A_2, Fig. 1) the minimization of the overall pressure drop ΔP_2 yields $(r_{i2}/r_{i1})_{opt} = 2^{3/7}$. The user temperature and total volume of insulation are

$$\theta_2 = \frac{T_{end} - T_\infty}{T_2 - T_\infty} = \theta_1 \exp\left(-\frac{N_0}{2\ln R_2} \right), \tag{13}$$

$$\tilde{V}_2 = \frac{V_2}{\pi L_0 r_{i0}^2} = \left(\frac{r_{i2}}{r_{i0}}\right)^2 (R_2^2 - 1) + 2\tilde{V}_1, \tag{14}$$

where $R_2 = (r_o/r_i)_2$. The maximization of θ_2 subject to the $\tilde{V}_2 = \text{constant}$ yields the optimal distribution of insulation reported in Fig. 3(a) and the end temperature shown in Fig. 3(b). The ratios $(R_0/R_1)_{opt} > 1$ and $(R_1/R_2)_{opt} > 1$ mean that the shells of insulation become relatively 'thin' when wrapped on the central ducts (stems) of larger and larger constructs. The constant value of $(\tilde{V}_1/\tilde{V}_2)_{opt}$ means that when the smallest pipe size r_{i0} is fixed, the amount of insulation allocated to each first construct (V_1) is a certain fraction of the total amount of insulation (V_2), independent of the size of V_2. The maximized end temperature increases as the total amount of insulation increases, and as the number of elemental heat loss units decreases (Fig. 3(b)).

The construction (assembly and optimization) detailed here for A_1 and A_2 was continued in the same manner up to A_4. In Section 4, the performance of the A_4 construct optimized in accordance with this section and Fig. 1 is compared with the performance of the construct of equal size obtained based on one-by-one addition of new users.

3. One-by-one tree growth

Consider now the alternative of adding new users to an existing structure, while not having the means to re-optimize the structure after the new users have been added. Furthermore, the addition of each new user is decided from the point of view of the user, not from the

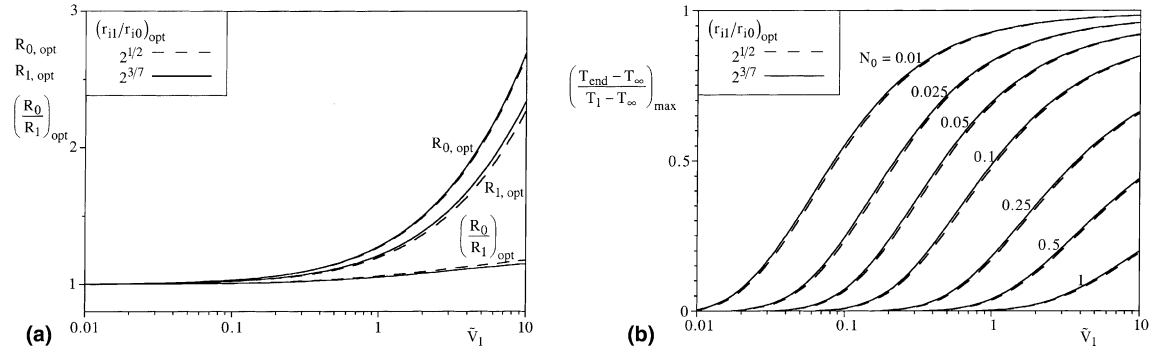

Fig. 2. The optimal ratios of insulation radii and the maximized end-user temperature for the first construct (A_1) of the pairing sequence (Fig. 1).

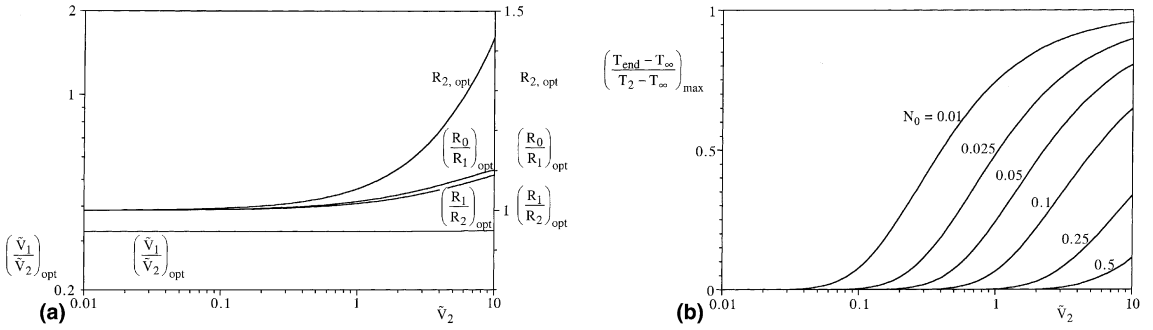

Fig. 3. The optimal ratios of insulation radii and the maximized end temperature for the second construct (A_2) of the pairing sequence (Fig. 1).

point of view of maximizing global performance. Each new user is connected to the tree network in the place that maximizes the user's benefit, namely, the temperature of the water stream that the new user receives.

In this new approach we must have a start, and for this we choose the optimized A_2 construct of Fig. 1, which is reproduced in Fig. 4. The A_2 construct has the area $4L_0^2$, and the property that its four users receive water at the same temperature, $T_1 = T_2 = T_3 = T_4$. The overall pressure drop has been minimized according to the pipe size ratios r_{i2}/r_{i1} and r_{i1}/r_{i0}. The total amount of insulation has been distributed optimally according to the insulation radii ratios R_0, R_1 and R_2.

Consider now the decision to add a new elemental user $(\dot{m}_0, L_0^2)$ to the A_2 construct. Because of symmetry, we recognize only the three possible positions (a,b,c) shown in Fig. 4. For the pipe that connects the new user to the existing A_2 construct we use the pipe size and insulation design of the elemental system of A_2, namely, r_{i0} and R_0. In going from the A_2 construct of Fig. 1 to the constructs of Fig. 4, the overall mass flow rate has increased from $4\dot{m}_0$ to $5\dot{m}_0$. The addition of the new user disturbs the optimally balanced distribution of resistances and temperatures, which was reached based on the analysis presented in the preceding section.

To deliver the hottest water from the network to the new user we must use the shortest pipe possible. By analyzing the user water temperature in the three configurations identified in Fig. 4 we find that $T_{5,b} > T_{5,a} > T_{5,c}$. For example, for the configuration of Fig. 4(a) it can be shown based on an analysis of the same type as in Eqs. (2)–(5) that the temperature of the hot water received by the new user (T_5) is

$$\frac{T_5 - T_\infty}{T_0 - T_\infty} = \exp\left(-\frac{5N_0}{2\ln R_0} - \frac{N_0}{3\ln R_1} - \frac{2N_0}{5\ln R_2} \right). \tag{15}$$

The corresponding expressions for the hot water temperature of the new user in the configurations of Figs. 4(b) and (c) are

$$\frac{T_5 - T_\infty}{T_0 - T_\infty} = \exp\left(-\frac{2N_0}{\ln R_0} - \frac{N_0}{3\ln R_1} - \frac{2N_0}{5\ln R_2} \right), \tag{16}$$

$$\frac{T_5 - T_\infty}{T_0 - T_\infty} = \exp\left(-\frac{3N_0}{\ln R_0} - \frac{2N_0}{5\ln R_2} \right). \tag{17}$$

These equations for T_5, and the corresponding expressions for the temperatures of the hot water streams received by the existing four users $(T_1, \ldots, T_4)$ are plotted in Fig. 5 for the same elemental number N_0. At first sight, these figures show the trend that is expected from Fig. 3(b): the temperature of the delivered water increases as the total mount of insulation $(\tilde{V}_2)$ increases. These figures, however, tell a more important story: they show not only how the choice of grafting (a,b,c) affects the temperature T_5, but also how the new (fifth) water stream affects the temperatures felt by the previous users.

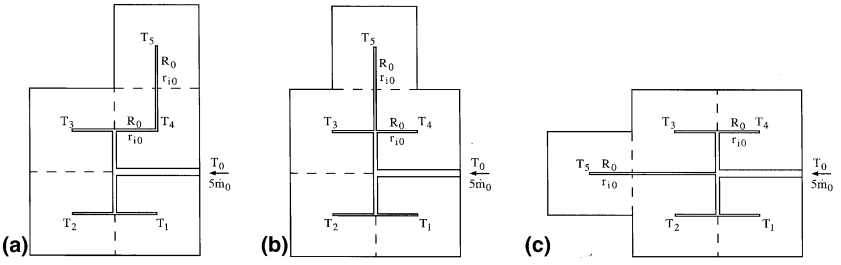

Fig. 4. Three possible ways of attaching a new user to the optimized A_2 construct of hot water pipes of Fig. 1.

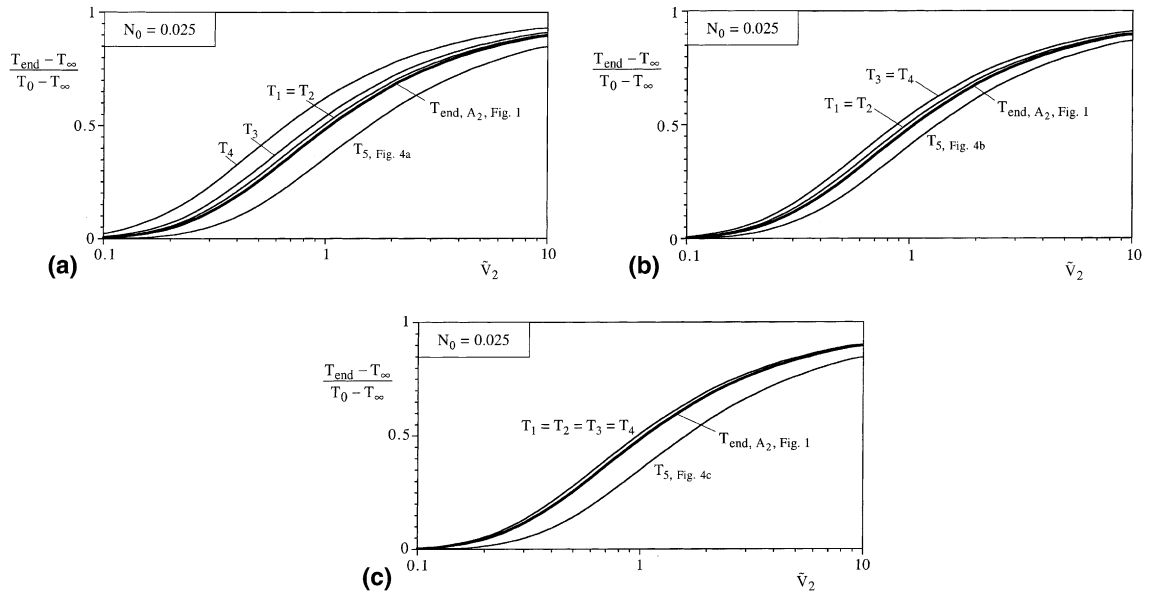

Fig. 5. The temperatures of the hot water delivered to the five users in the configurations of Fig. 4(a), Fig. 4(b), and Fig. 4(c).

Before the fifth user was added, the constructal design of A_2 delivered water of the same temperature to the four users. Note the single curve drawn for $T_{\text{end, } A_2, \text{ Fig. 1}}$ in each of the graphs of Fig. 5. This curve serves as reference in each of the designs of Fig. 4, where the temperatures of the existing users are altered by the insertion of a fifth user. In the configuration of Figs. 4(a) and 5(a), the fifth-user temperature drops below the original temperature of hot water delivery ($T_{\text{end, } A_2, \text{ Fig.1}}$). In the same design, the temperatures of the four older users increase, the largest increases being registered by the users that are situated the closest to the newly added user. It is as if the new user insulates (or shields) its closest neighbors from cold water. It does so by drawing a larger stream of hot water in its direction and in the direction of its immediate neighbors.

These features are also visible in the performance of the configurations of Figs. 4(b) and (c) (cf. Fig. 5(b) and (c)), but the differences between the water temperatures of the five users are not as great as in the case of Fig. 4(a) (Fig. 5(a)). It is interesting that the best configuration (Figs. 4(b) and 5(b)), where the water received by the new user is the hottest, is also the configuration in which all the users receive water at nearly the same temperature. This finding is in line with the seemingly general conclusion that the optimal design of a complex flow system is the one where the imperfections are distributed as uniformly as possible [1]. In the class of problems treated here, by imperfections we mean the decrease of the hot water temperature, which is due to the loss of heat to the ambient across the insufficient (finite) amount of insulation. This point is stressed further by Fig. 5(c), which shows that the water temperatures of the four existing users are affected in equal measure by the insertion of the fifth user. The symmetry in this case is explained by the fact that in Fig. 4(c) the new user is attached to the hub of the previously optimized A_2 construct, at equal distance away from the existing four users.

The relative lack of success of design (c) in Fig. 4 may be attributed at first sight to the fact that the new user requires a longer pipe ($1.5L_0$) for its connection to the original construct, whereas in designs (a) and (b) the required connection is shorter (L_0). This explanation is not as straightforward as this, because design (c) has the advantage that the new user is connected to the heart (hot region) of the construct, while in designs (b) and (c) the new user is connected to peripheral locations. This competition between the length of the link and the temperature of the point of attachment to the original structure make the entire procedure subtle, i.e., not transparent. It is necessary to try all the possible configurations before deciding which design step, or rule is beneficial.

In conclusion, we retain the design of Fig. 4(b), and proceed to the next problem, which is the placing of a new (sixth) user in the best spot on the periphery of the five-user construct. The two most promising choices are shown in Fig. 6. They are the most promising because in each case the new user is attached to a source with relatively high temperature. In other words, unlike in Fig. 4 where we considered without bias all the possible ways of attaching the fifth user, now and in subsequent steps

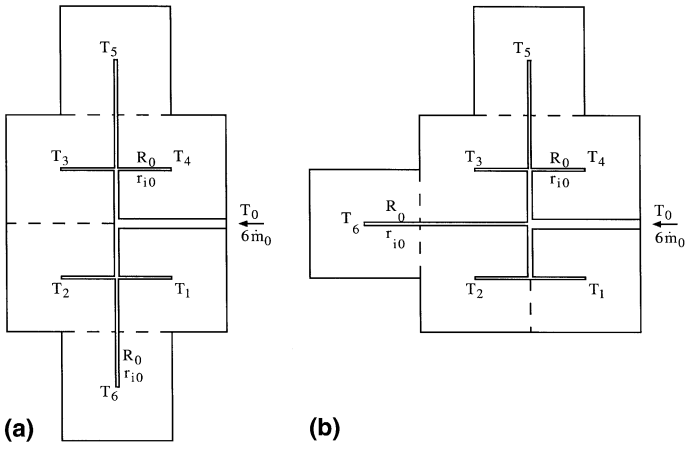

Fig. 6. Two ways of attaching a sixth user to the construct selected in Fig. 4(b).

of growing the structure we expedite the place-selection process by using conclusions and trends learned earlier. For brevity, we also omit the analytical description of the type shown in Eqs. (15)–(17).

The performance curves plotted in Fig. 7 reinforce some of the earlier trends. Fig. 7(a) shows that when the new user is placed symmetrically relative to the fifth user (Fig. 6(a)), symmetry is preserved in the temperature distribution over the entire tree. Note that in this configuration T_6 equals T_5. Symmetry works in favor of making the distribution of temperature (and heat loss, imperfection) more uniform.

The competing configuration (Fig. 6(b)) has the new user attached to the center of the original A_2 construct, in the same place as in Fig. 4(c). Its performance is documented in Fig. 7(b). The configuration of Fig. 6(b) is inferior to that of Fig. 6(a) because the temperature T_6 of Fig. 7(b) is consistently lower than the corresponding temperature of Fig. 7(a). Furthermore, the configuration of Fig. 6(b) is inferior because it enhances the nonuniformity in the temperature of the water received by all the users.

In sum, we retain the configuration of Fig. 6(a) for the construct with six users. It is important to note that this is the first instance where the symmetrical placement of the even-numbered user emerges as the best choice. This conclusion was tested (one new user at a time) up to the 12th new user, beyond which it was adopted as a rule for expediting the optimized growth of structure. In other words, each even-numbered new user was placed symmetrically relative to the preceding odd-numbered user (the placement of which was optimized).

Fig. 8 shows the three most promising positions that we tried for a new seventh user. Temperature distribution charts (such as Fig. 7) were developed for each configuration, but are not shown. On that basis we found that the seventh-user temperature T_7 decreases, in order, from Fig. 8(b) to Fig. 8(a), and finally to Fig. 8(c). We retained the configuration of Fig. 8(b), and proceeded to the selection of the best place for an eight user. The best position for the eight user is the symmetric arrangement shown in Fig. 9(a). The rest of Fig. 9 shows the optimal positioning of subsequent users up to the sixteenth. The rule that is reinforced by these choices is

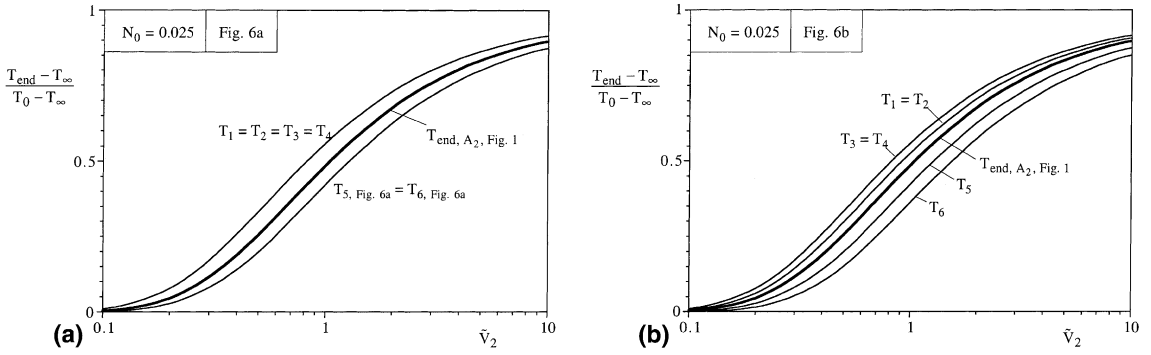

Fig. 7. The temperatures of the hot water delivered to the fifth and sixth users in the configurations of Figs. 6(a) and (b).

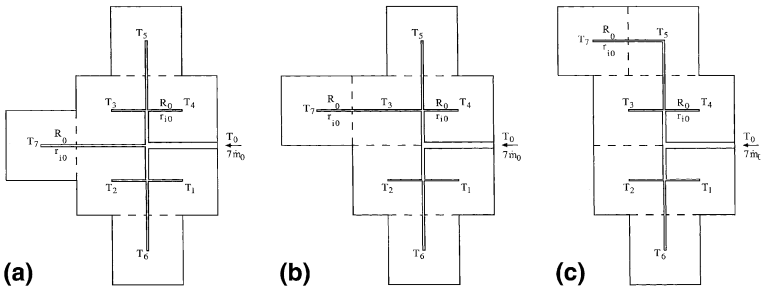

Fig. 8. Three ways of placing a seventh user in the construct selected in Fig. 6(a).

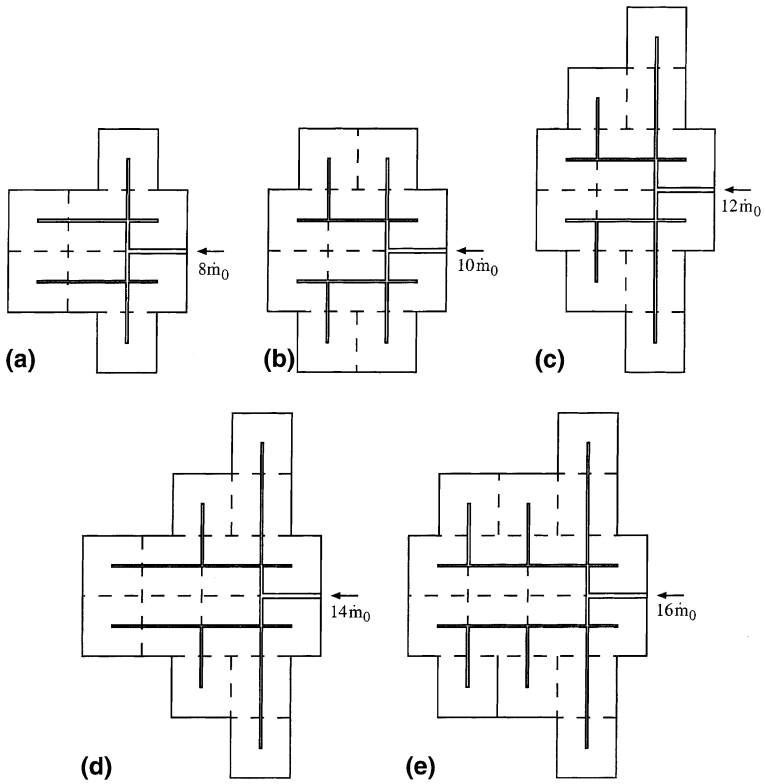

Fig. 9. The best configurations for the constructs with users from 8 to 16.

that the better position for a new user is that one that requires a short connection to that side of the existing construct where the water delivery temperatures are higher.

4. Discussion: complex structures are efficient and robust

We are now in a position to compare the performance of designs based on one-by-one growth (Fig. 9) with the constructal designs obtained by repeated doubling (Fig. 1). The most complex design of the one-by-one sequence (Fig. 9(e)) is compared with its constructal counterpart in Fig. 10(a). The comparison is done on the same basis, that is, the same total amount of insulation material, and the same serviced territory ($16L_0^2$). We see that the excess temperature of the latest (16th) user in Fig. 9(e) is consistently less than the excess temperature felt by each of the users in A_4 construct generated by doubling (recall that in Fig. 1 each user receives water at the same temperature).

The discrepancy between the performances of the two designs compared in Fig. 10(a) diminishes as the total amount of insulation ($\tilde{V}_{A_{16}}$, Fig. 9(e)) increases, and

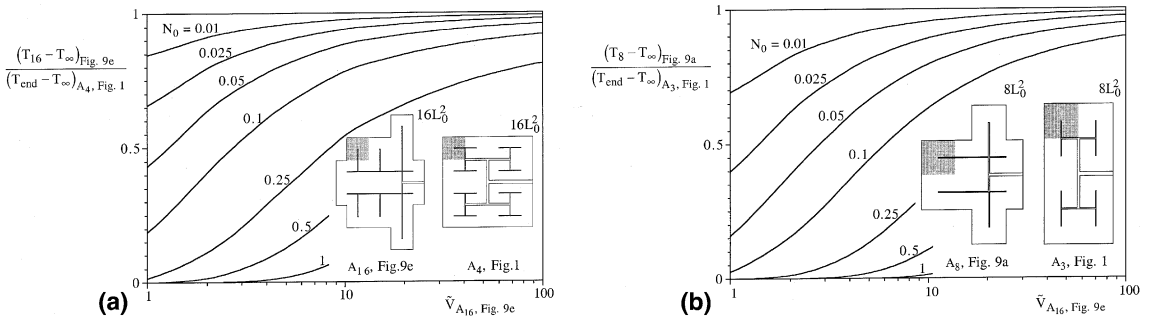

Fig. 10. (a) Comparison between the excess temperature of the water received by the last user added to the structure of Fig. 9(e), and the corresponding temperature in the design based on the sequence of Fig. 1. (b) Comparison between the excess temperature of the water received by the last user added to the structure of Fig. 9(b), and the corresponding temperature in the design based on the sequence of Fig. 1.

as N_0 decreases. The smaller N_0 corresponds to better insulation materials (smaller k) and denser populations of users (smaller L_0). An important question is how this discrepancy depends on the complexity of the flow structure. Is it always important to strive for the best (e.g., Fig. 1), or will an on-the-spot optimization (e.g., Fig. 9) be sufficient?

We examined this question by changing the complexity of the structure, and repeating the test of Fig. 10(a). The new structures are simpler, with only eight users. The one-by-one construction of Fig. 9(a) is compared with the A_3 design of the sequence shown in Fig. 1. The comparison shown in Fig. 10(b) is for the same territory ($8L_0^2$) and total amount of insulation material. The trends are the same as what we saw in Fig. 10(a). The excess water temperature $(T_8 - T_\infty)$ of the last user added to Fig. 9(a) is consistently lower than what the users of the constructal design receive.

An important observation is that the ratio $(T_8 - T_\infty)/(T_{\text{end}} - T_\infty)$ of Fig. 10(b) is consistently lower than the corresponding ratio $(T_{16} - T_\infty)/(T_{\text{end}} - T_\infty)$ of Fig. 10(a). 'Corresponding' means that the total amount of insulation material and the serviced territory are the same in both figures. The same territory means that $16L_{0,\ \text{Fig.10(a)}}^2 = 8L_{0,\ \text{Fig.10(b)}}^2$ or that the L_0 scale of the constructs of Fig. 10(b) exceeds by a factor of $2^{1/2}$ the L_0 dimension of the constructs of Fig. 10(a). In both designs, the individual user receives the flowrate $\dot{m}_0$.

This observation is reinforced by Fig. 11(a), which shows the same comparison for a structure with only four users. The constructal design is A_2 of Fig. 1. The corresponding one-by-one design is shown on the left side. The total insulation volume $(\tilde{V})$ and serviced territory $(4L_0^2)$ is the same in both designs. The one-by-one structure approaches the performance of the constructal design as N_0 decreases and $\tilde{V}$ increases. To test the effect of complexity, which decreases from Fig. 10(a) to (b) and, finally, to Fig. 11(a), we must put all the designs on the same $\tilde{V}$ and A basis. This means that the territory covered by four users in the designs of Fig. 11(a) is covered by 16 users in the designs of Fig. 10(a). Consequently, the L_0 scale in Fig. 11(a) is twice the L_0 scale of Fig. 10(a). The same proportionality exists between the respective N_0 values.

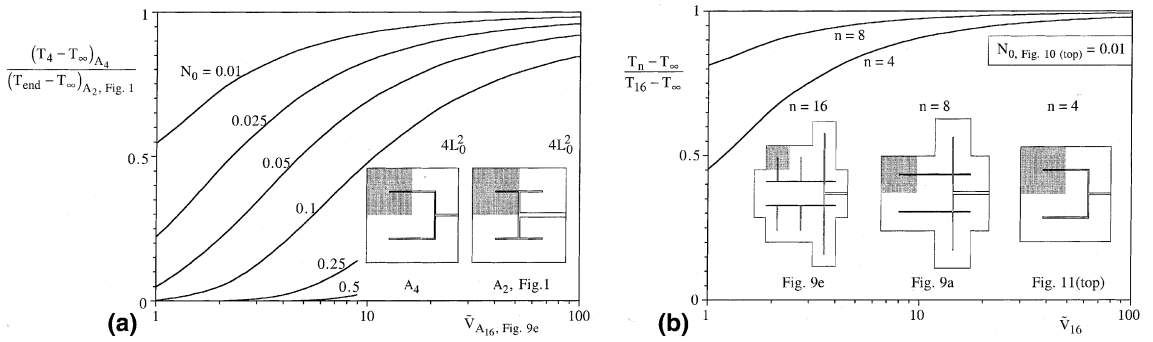

Fig. 11. (a) Comparison between the excess temperature of the water received by the last user added to a structure with four users, and the corresponding temperature in the design (A_2) based on the sequence of Fig. 1. (b) Comparison between the one-by-one designs of Figs. 10 and 11, showing how the performance improves as the complexity (n) increases.

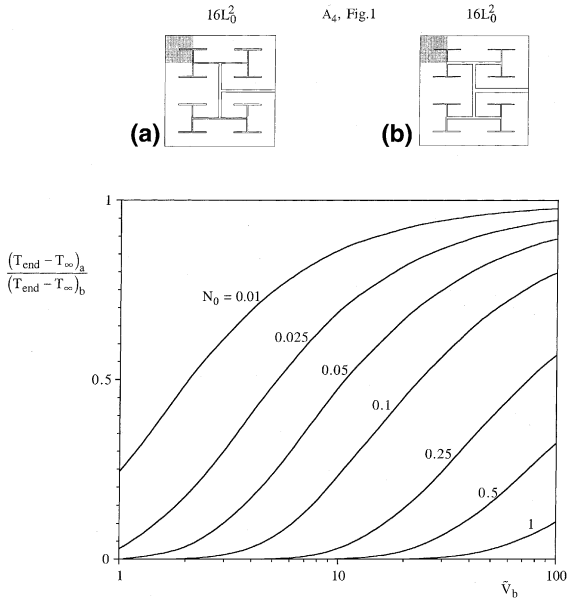

Fig. 12. The effect of optimizing the distribution of insulation over (a) three pipe sizes vs. (b) five pipe sizes, in the A_4 design of the sequence of Fig. 1.

In summary, the performance of the structure increases as its complexity increases. Fig. 11(b) brings together the one-by-one designs of Figs. 10 and 11. They cover the same area A, which means that the L_0 scale of the users in Fig. 9(e) ($n = 16$) is the shortest. The $n = 16$ design is used as reference. The three designs use the same amount of insulation material. The k and $\dot{m}_0$ values are such that the N_0 value [Eq. (5)] based on the L_0 length of the $n = 16$ case of Fig. 10(a) is $N_0 = 0.01$. Fig. 11(b) shows that the end-user water excess temperature increases as the complexity of the structure (n) increases.

A major limitation of the one-by-one design is the memory that is built into the system. Memory is reinforced at every step. What was built prior to the insertion of the last user is retained. This is why in the one-by-one sequence of Fig. 9 there are only three sizes of pipes and their insulations: the three sizes that were inherited in the first step (Fig. 4), from the A_2 construct of Fig. 1. In a complete optimization of a multiscale flow structure, there is an optimal pipe size for every level of branching and coalescence. This means that the existence of only three pipe sizes in structures as complex as those exhibited in Fig. 9 is a departure from the best possible performance.

The extent of this departure is illustrated in Fig. 12. Here the area size ($16L_0^2$), insulation material ($\tilde{V}$) and complexity ($n = 16$) are fixed. We used the A_4 construct of Fig. 1 in two settings, the design (b) with every pipe size optimized, and the design (a) with the only three sizes that were available at the A_2 level. Fig. 12 shows convincingly that design (b) is better, however, the difference between (a) and (b) is not great when N_0 is of order 0.01, and the amount of insulation is large enough. Compare the high position of the $N_0 = 0.01$ curve in Fig. 12 with the positions of the same N_0 curve in earlier figures, e.g. Fig. 10(a): the design of Fig. 9(e) is superior to that of Fig. 12(a).

In conclusion, the design of the insulated structure is robust with respect to how the insulation is distributed over all the pipes. The performance of the structure (how well it services the end user) is relatively insensitive to how finely the distribution of pipe sizes and insulation radii is optimized.

Acknowledgements

This work was supported by the National Science Foundation. Mr. Wechsatol also acknowledges the support received from King Mongkut's University of Technology (KMUTT), Thailand.

References

[1] A. Bejan, Shape and Structure, from Engineering to Nature, Cambridge University Press, Cambridge, UK, 2000.
[2] E.R. Weibel, Morphometry of the Human Lung, Academic Press, New York, 1963.
[3] A.E. Scheidegger, Theoretical Geomorphology, second ed., Springer, Berlin, 1970.
[4] N. MacDonald, Trees and Networks in Biological Models, Wiley, Chichester, UK, 1983.
[5] H.L. Willis, W.G. Scott, Distributed Power Generation, Marcel Dekker, New York, 2000.
[6] W. Aung (Ed.), Cooling Technology for Electronic Equipment, Hemisphere, New York, 1988.
[7] G.P. Peterson, A. Ortega, Thermal control of electronic equipment and devices, Adv. Heat Transfer 20 (1990) 181–314.
[8] S. Kakac, H. Yüncü, K. Hijikata (Eds.), Cooling of Electronic Systems, Kluwer Academic Publishers, Dordrecht, The Netherlands, 1994.
[9] A. Bar-Cohen, W.M. Rohsenow, Thermally optimum spacing of vertical, natural convection cooled, parallel plates, J. Heat Transfer 106 (1984) 116–123.
[10] R.W. Knight, J.S. Goodling, D.J. Hall, Optimal thermal design of forced convection heat sinks – analytical, J. Electron. Packaging 113 (1991) 313–321.
[11] N.K. Anand, S.H. Kim, L.S. Fletcher, The effect of plate spacing on free convection between heated parallel plates, J. Heat Transfer 114 (1992) 515–518.
[12] A. Bejan, Constructal-theory network of conducting paths for cooling a heat generating volume, Int. J. Heat Mass Transfer 40 (1997) 799–816.
[13] C. Martinand, Le Génie Urbain Rapport au Ministre de l'Equipement, du Logement, de l'Aménagement du Terri-

toire et des Transports, La Documentation Francaise, Paris, 1986.
[14] J. Bastié, B. Dézert, L'Espace Urbain, Masson, Paris, 1980.
[15] J. Pelletier, C. Delfante, Villes et Urbanisme dans le Monde, Masson, Paris, 1989.
[16] J. Padet, Fluids en Écoulement. Méthodes et Modèles, Masson, Paris, 1991.
[17] A. Dupont, Hydraulique Urbaine, Ouvrages de Transport, Elévation et Distribution, Eyrolles, Paris, 1977.
[18] J. Bonnin, Hydraulique Urbaine Appliquée aux Agglomérations de Petite et Eyrolles, Eyrolles, Paris, 1977.
[19] P. Nonclercq, Hydraulique Urbaine Appliquée, CEBEDOC, Liège, 1982.
[20] M. Falempe, Une plate-forme d'enseignement et de recherche du procédé de cogénération chaleur-force par voie de vapeur d'eau, Revue Générale de Thermique 383 (1993) 642–651.
[21] M. Falempe, B. Baudoin, Comparaison des dix méthodes de résolution des réseaux de fluides à usages énergétiques, Revue Générale de Thermique 384 (1993) 669–684.
[22] A. Barreau, J. Moret-Bailly, Présentation de deux méthodes d'optimisation de réseaux de transport d'eau chaude à grande distance, Entropie 75 (1977) 21–28.
[23] B. Plaige, Le Chauffage Urbain en Pologne, Chauffage, Ventilation, Conditionement d'Air No. 9 (1999) 19–23.
[24] W.J. Wepfer, R.A. Gaggioli, E.F. Obert, Economic sizing of steam piping and insulation, J. Eng. Ind. 101 (1979) 427–433.
[25] A. Bejan, G. Tsatsaronis, M. Moran, Thermal Design and Optimization, Wiley, New York, 1996.